



## Article

# Characterizing a Newly Designed Steel-Wool-Based Household Filter for Safe Drinking Water Provision: Hydraulic Conductivity and Efficiency for Pathogen Removal

Raoul Tepong-Tsindé <sup>1</sup>, Arnaud Igor Ndé-Tchoupé <sup>2</sup> , Chicgoua Noubactep <sup>1,\*</sup> , Achille Nassi <sup>2</sup> and Hans Ruppert <sup>3,\*</sup>

<sup>1</sup> Department of Applied Geology, University of Göttingen, Goldschmidtstraße 3, D-37077 Göttingen, Germany; raoultepong@googlemail.com

<sup>2</sup> Department of Chemistry, Faculty of Sciences, University of Douala, B.P. Douala 24157, Cameroon; ndetchoupe@gmail.com (A.I.N.-T.); achillen@yahoo.fr (A.N.)

<sup>3</sup> Department of Sedimentology & Environmental Geology, University of Göttingen, Goldschmidtstraße 3, D-37077 Göttingen, Germany

\* Correspondence: cnoubac@gwdg.de (C.N.); hruppert@gwdg.de (H.R.)

Received: 23 November 2019; Accepted: 16 December 2019; Published: 17 December 2019



**Abstract:** This study characterizes the decrease of the hydraulic conductivity (permeability loss) of a metallic iron-based household water filter (Fe<sup>0</sup> filter) for a duration of 12 months. A commercial steel wool (SW) is used as Fe<sup>0</sup> source. The Fe<sup>0</sup> unit containing 300 g of SW was sandwiched between two conventional biological sand filters (BSFs). The working solution was slightly turbid natural well water polluted with pathogens (total coliform = 1950 UFC mL<sup>-1</sup>) and contaminated with nitrate ([NO<sub>3</sub><sup>-</sup>] = 24.0 mg L<sup>-1</sup>). The system was monitored twice per month for pH value, removal of nitrate, coliforms, and turbidity, the iron concentration, as well as the permeability loss. Results revealed a quantitative removal of coliform (>99%), nitrate (>99%) and turbidity (>96%). The whole column effluent depicted drinking water quality. The permeability loss after one year of operation was about 40%, and the filter was still producing 200 L of drinking water per day at a flow velocity of 12.5 L h<sup>-1</sup>. A progressive increase of the effluent pH value was also recorded from about 5.0 (influent) to 8.4 at the end of the experiment. The effluent iron concentration was constantly lower than 0.2 mg L<sup>-1</sup>, which is within the drinking-water quality standards. This study presents an affordable design that can be one-to-one translated into the real world to accelerate the achievement of the UN Sustainable Development Goals for safe drinking water.

**Keywords:** biosand filter; household filter; pathogen removal; permeability loss; zero-valent iron

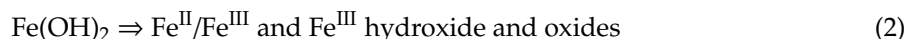
## 1. Introduction

Accelerating universal access to safe drinking water (and sanitation) is the aim of the United Nations Sustainable Development Goals (SDG's six) [1,2]. "Leaving no one behind" without safe drinking water can only be achieved if efficient and affordable technologies are made available to people where they are currently living, including in their remote and scattered rural homes and in slums of crowded cities. Clearly, decentralized solutions, such as small-scale water treatment units, are needed [3–5]. Water filtration on granular Fe<sup>0</sup> beds has been demonstrated to be one such affordable technology [2,6–9]. However, the large-scale implementation of Fe<sup>0</sup> filters is impaired by several operational factors of which the decrease of the hydraulic conductivity (permeability loss) is the most crucial [10–12].

Gravity-driven  $\text{Fe}^0$  filters can be constructed, operated, and maintained by users with relatively low technical skills [13,14]. The present work is a part of an effort to facilitate the design of compact household  $\text{Fe}^0$  filters for the population of urban slums, taking Douala (Cameroon) as a model city [15]. Several conceptual filters were already discussed [16]. The present work presents the current state of efforts to characterize the longevity of a steel wool (SW)-based  $\text{Fe}^0$  filter in terms of permeability loss.

The tested water treatment train was conceptually derived from the seminal work of Westerhoff and James [16,17], wherein filtration is performed on a series of beds containing granular materials and including at least one biological sand filter (BSF) and one  $\text{Fe}^0$ /sand filter. BSFs preceding the  $\text{Fe}^0$ /sand filter(s) are designed to remove suspended solids by straining (size exclusion) and pathogens by metabolic breakdown, natural death, and predation [18,19]. However, because specific biological processes may also generate metal oxides and organic matter, quantitative scavenging chemical pollutants in BSFs have also been reported [20]. In this study, the removal of chemicals is mainly attributed to iron corrosion within  $\text{Fe}^0$ /sand columns [9,16]. BSFs coming after the  $\text{Fe}^0$ /sand filter(s) act as a scavenger of dissolved Fe and can be regarded in the long-term as iron-oxide-coated sand units, able to remove pathogens and chemicals [21,22]. Clearly, the removal of pathogens and chemical contaminants in such designs is certain. The research question is how to design an efficient and sustainable system [8]. The main incertitude relies on the long-term permeability [23,24].

The incertitude on the long-term permeability of  $\text{Fe}^0$  filters arises from the evidence that aqueous iron corrosion is a volumetric expansive process [25]. In fact, immersed  $\text{Fe}^0$  corrodes after reaction 1 (Equation (1)), and  $\text{Fe}(\text{OH})_2$  is further transformed to various iron hydroxides and oxides (Equation (2)) [26]. Each iron oxide is larger in volume than the metallic iron ( $V_{\text{oxide}} > V_{\text{iron}}$ ) [25–27].



Equations (1) and (2) imply that, at pH values of natural waters,  $\text{Fe}^0$  can universally be used to produce  $\text{H}_2$  and iron hydroxides/oxides. However, the kinetics and the extent of the generation of iron oxides have not been properly considered in past efforts [24,28,29]. On the other hand, it is known that: (i) the kinetics of iron corrosion are never linear [28–30], (ii) the size of  $\text{Fe}^0$  particles is a relevant parameter for the corrosion kinetics [22,23], and (iii) the service life of a hybrid  $\text{Fe}^0$  filter depends on its  $\text{Fe}^0$  content and the proportion of  $\text{Fe}^0$  in the (homogeneous) mixture [26].

Reports found in the literature on using  $\text{Fe}^0$  SW for water treatment clearly demonstrate the need for systematic investigation to design sustainable SW-based filters [31]. For example, the filters of Laudale and Emmons [3] containing a pure  $\text{Fe}^0$  SW layer were not sustainable (permeability loss). On the other hand, systems with SW ratios lower than 10% (w/w) have not experienced any permeability loss [32,33]. The region between 10% and 100%  $\text{Fe}^0$  SW (w/w) in filtration systems is yet to be investigated. It is theoretically established [27] and experimentally confirmed [34] that lower  $\text{Fe}^0$  ratios warrant a system's sustainability (long-term permeability) while higher  $\text{Fe}^0$  ratios care for higher efficiency. Thus, having an appropriate balance between reactive  $\text{Fe}^0$  and a less or non-reactive aggregate (e.g., gravel, pumice, sand) is essential for an efficient and sustainable  $\text{Fe}^0$  filter [23].

Insufficient information is available to determine the feasibility of using  $\text{Fe}^0$  SW to design a household water filter. Despite its worldwide availability, steel wool has only been scarcely tested for situations applicable to decentralized safe drinking water provision [22,35–39]. Among these works, only the last two referenced performed column studies. Rao and Murthy [39] filled the hollow portion of an existing domestic candle filter with  $\text{Fe}^0$  SW (100%) and tested its suitability for As removal. Bradley et al. [22] mixed 260 g of a  $\text{Fe}^0$  SW (extra fine or grade 0000) with sieved sand (effective size 0.4 mm) to form a 20 cm-thick filter for virus removal for 300 days (10 months). The authors reported that the used SW ( $d_1 = 25 \text{ mm}$ ) was completely depleted after 170 days (8 months) while the system was still permeable. On the contrary, George and Ahammed [40] tested a filter containing iron nails ( $d_2 = 2.0 \text{ mm}$ ) for just four months and did not consider Bradley et al. [22] while discussing their

results. Using a larger particle ( $d_2/d_1 = 80$ ) and testing it for a shorter experimental duration ( $t_1/t_2 = 2.5$ ) is counter-intuitive, particularly in a context where long-term experiments are needed [2,9]. There is a need to further investigate the relationship between SW proportion in a  $\text{Fe}^0$  filter, its long-term permeability and its efficiency for water treatment [19,41,42].

The objective of this work was to characterize long-term changes of the hydraulic conductivity (permeability loss) of a newly designed  $\text{Fe}^0$  SW household water filter. The tested  $\text{Fe}^0$  SW filter is considered as a “black box” made up of three columns (Figure 1). The compact system comprised a  $\text{Fe}^0$ /sand filter sandwiched between two biological sand filters (BSF) and was intermittently fed by natural well water. The well water was slightly turbid, polluted with pathogens, and contaminated with  $\text{NO}_3^-$ . The experiment lasted for one year.

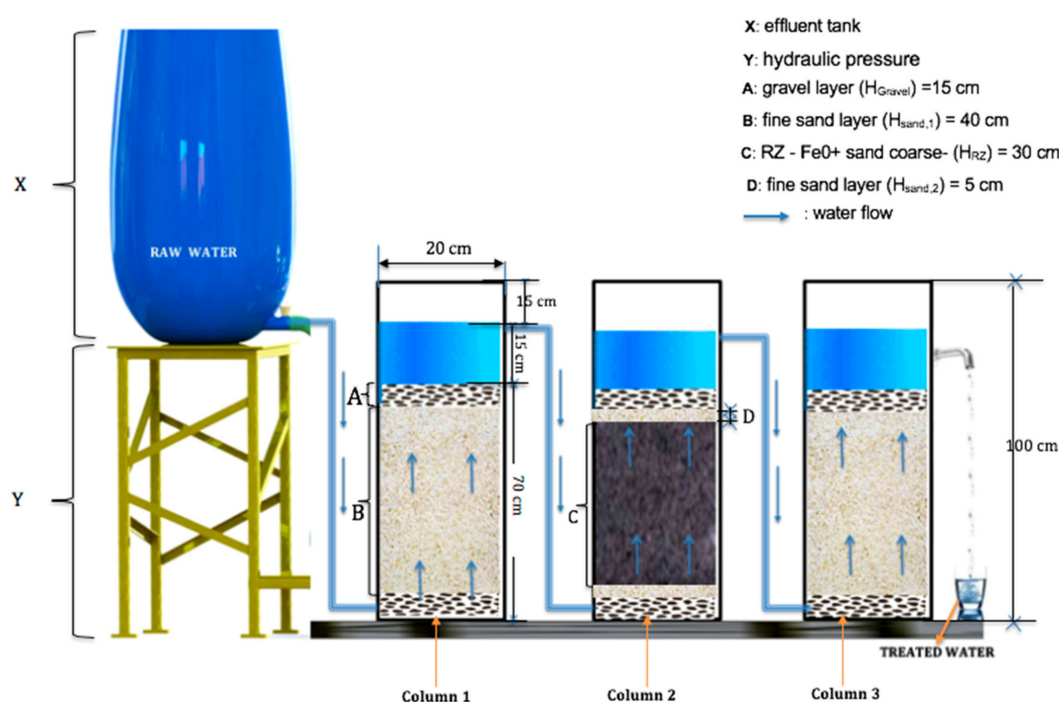


**Figure 1.** Schematic diagram of the designed filtration system. Well water was stored in a 200 L tank. The first and the third columns are conventional biosand filters (BSFs). The column in the middle is the  $\text{Fe}^0$  steel wool (SW) unit. The columns are connected to each other with a PET tube.

## 2. Materials and Methods

### 2.1. Filter Characteristics

The tested design is made up of three identical cylindrical Plexiglass columns (length: 100 cm; inner diameter: 20.0 cm) mounted in series—two conventional BSFs and one  $\text{Fe}^0$  SW unit in between. Upon successful testing, the unit is intended to be transferred for use in households, but with a proper housing (e.g., concrete material). The test device was constructed inside a room of the Institute of Applied Technology in Douala (Cameroon). The used room was not a conventional experimental laboratory but offered representative conditions for a household situation. The room temperature range was  $26 \pm 2$  °C.

The columns were connected to each other by using a 1.5 m PET (poly-ethylene terephthalate) tube of 2.4 cm inner diameter. The columns were packed from the bottom to the top as follows (Table 1): (i) 15.0 cm gravel ( $H_{\text{gravel},1}$ ), (ii) 40.0 cm of a reactive zone, and (iii) 15.0 cm gravel layer ( $H_{\text{gravel},2}$ ). For column 1 and 3, the reactive zone was a fine sand layer ( $H_{\text{sand},1}$ ). For column 2, the 40 cm was filled with a 30.0 cm reactive zone ( $H_{\text{rz}}$ ) made up of a mixture of  $\text{Fe}^0$  SW and coarse sand ( $\text{Fe}^0$ /sand) and sandwiched between two 5.0 cm fine sand layers ( $H_{\text{sand},2}$ ).

**Table 1.** Summary of the used experimental setup.  $H_{\text{gravel1}}$  and  $H_{\text{gravel2}}$  are the heights of the underdrain and the upper layer, respectively;  $H_{\text{sand1}}$  and  $H_{\text{sand2}}$  the heights of fine sand;  $H_{\text{sand}}$  is the fine sand layer; and  $H_{\text{RZ}}$  is the height of the reactive layer ( $\text{Fe}^0/\text{sand}$  coarse).

Designation	Height (cm)		
	Column 1	Column 2	Column 3
Gravel ( $H_{\text{gravel1}}$ )	15.0	15.0	15.0
Sand ( $H_{\text{sand2}}$ )	-	5.0	-
Sand ( $H_{\text{sand1}}$ )	40.0	-	40.0
RZ ( $\text{Fe}^0/\text{coarse sand}$ ) ( $H_{\text{RZ}}$ )	-	30.0	-
Sand ( $H_{\text{sand2}}$ )	-	5.0	-
Gravel ( $H_{\text{gravel2}}$ )	15.0	15.0	15.0

The total depth of materials in each column was 70.0 cm.

The reactive layer was prepared by carefully introducing sand grains and chopped  $\text{Fe}^0$  SW in small lofts into the column. The  $\text{Fe}^0/\text{sand}$  mixture (10% SW—vol/vol) was previously mixed in a large beaker. Once in the column, water was added to the mixture and it was gently compacted by manual tapping using a 100 mL PET bottle filled with water. The 300 g of  $\text{Fe}^0$  SW and 14,200 g of coarse sand had a corresponding  $\text{Fe}^0$  weight ratio of 2.07%. Bradley et al. [22] also reported on such a low weight percentage of  $\text{Fe}^0$  SW in a  $\text{Fe}^0/\text{sand}$  filter. This is justified by the very low density of SW (low weight and large volume). To build a 20 cm reactive layer under their experimental conditions, Bradley et al. [22] used 260 g of  $\text{Fe}^0$  SW.

## 2.2. Media and Their Preparation for Filter

### 2.2.1. Sand

The used sand was a natural material from the Mungo River (Cameroon). Mungo sand was selectively sieved, using a set of sieves for sand analysis. The portion passing through a 1.0 mm sieve and retained by a 0.200 mm sieve was used as filter media in the BSFs and to build the separation layers ( $H_{\text{sand1}}$  and  $H_{\text{sand2}}$ ). Coarse sand (1.00–4.00 mm) was mixed with  $\text{Fe}^0$  SW to build the reactive zone. The original Mungo sand was washed several times using tap water until the wash water became clear. Retained fractions were separately warmed in boiling water for about 3.0 h. The sand was further dried in the sun for about 6.0 h. Sand was used because of its worldwide availability and its use as a typical admixing agent in  $\text{Fe}^0/\text{H}_2\text{O}$  systems [17,43].

### 2.2.2. Gravel

The used gravel (4.00–8.0 mm) was a natural material from a small river located in the vicinity of the University of Douala. Gravel was pre-treated like coarse sand and used as supporting layer and top layer in individual columns. The bottom gravel layer stores solids removed from raw water entering the first column (Figure 1). Gravel also prevents sand particles from falling and obstructing the inlet pipe.

### 2.2.3. Metallic Iron

A fine-grade  $\text{Fe}^0$  SW (grade 0) from “Grand Menage” trademark brand purchased in Douala (Cameroon) was used. Its average elemental composition was not determined as it was proven to not be a stand-alone determining reactivity parameter for  $\text{Fe}^0$  in general. Recently, Lufingo et al. [31] presented the first systematic study comparing the intrinsic reactivity of  $\text{Fe}^0$  SW. The elemental composition (%) of the grade 0 ( $d = 50 \mu\text{m}$ ) material they tested was: Fe: 99.08; Co: 0.05; Cu: 0.27; Ni: 0.11; and Cr: 0.49.

Fe<sup>0</sup> SW was chopped in sections of 1.0 to 5.0 mm length to use as a generator of iron hydroxides for contaminant scavenging [8,21,44].

### 2.3. Experimental Procedure

An intermittent gravity-driven filtration was performed for one year. Each filtration event was initiated by opening the outlet-controlled tap connected to column 1 and allowing the stored well water from the reservoir to flow through the entire system (Figure 1). Experiments were conducted on a daily basis from Monday to Friday. Two hundred liters of water was filtered per filtration event. Raw water was collected from a well used for drinking and other domestic purposes (Table 2). The well water was polluted with microorganisms; there was no need for artificially seeding it. The volume of effluent recorded during the first 10 min was used to calculate the flow velocity. At the end of the filtration event, the reservoir was immediately refilled with 200 L well water. The initial flow rate was 0.34 L min<sup>-1</sup> (20.40 L h<sup>-1</sup>) and was not further modified. This approach perfectly mimics pilot-scale intermittent filtration using household filters for daily water need in low-income communities. Previous investigations on lab-scale using gravity-fed systems also filtered a constant volume daily [45,46]. In such an approach, changes in flow velocity are observed through variations of the recorded water volume during the fixed time (herein, 10 min). The pH value, the iron level, and the extent of water decontamination were monitored. Complete water analysis including for pathogen was performed twice per month at the Centre Pasteur in Douala.

**Table 2.** Average composition of the used well water. The well is polluted with coliforms and depicts high levels of conductivity and turbidity compared to the WHO guidelines [1]. WHO stands for World Health Organization.

Parameter	Unit	Well Water	WHO (Guideline)
Turbidity	(NTU)	35 ± 2	<5
Conductivity	(μS cm <sup>-1</sup> )	296 ± 7	250
Total Iron	(mg L <sup>-1</sup> )	1.45 ± 0.25	<0.2
Nitrate	(mg L <sup>-1</sup> )	23.5 ± 4.5	<50
pH value (25 °C)	(-)	4.9 ± 0.2	6.5–8.5
Total coliform (TC)	(UFC mL <sup>-1</sup> )	1948.6 ± 45	0.0
Fecal coliforms (FC)	(UFC mL <sup>-1</sup> )	1495.0 ± 97	0.0

#### 2.3.1. Sample Collection

The 1 L sample bottles were provided by the Laboratory at the Centre Pasteur du Cameroon (Douala) and used to collect water samples from the filter twice per month for microbial analysis. These samples included the raw water from a private well (Table 2). The time from sample collection and transportation to the lab was less than 4 hours. It is considered that the effects of time and temperature on microbial survival is negligible.

#### 2.3.2. Efficiency Characterization

The efficacy of the designed filter to treat water was accessed by the extent of reducing the concentration of fecal coliform (FC) and total coliform (TC). In addition, turbidity, permeability loss, nitrate, and iron concentration were monitored.

### 2.4. Analytical Method

Iron concentrations were determined by using a UV–Vis spectrophotometer (Dr. Lange CADAS 200 LPG 392). The working wavelength was 510 nm. A cuvette with 1.0 cm light path was used. The iron determination followed the O-Phenanthroline method [47,48]. The spectrophotometer was calibrated for iron concentrations ≤10.0 mg L<sup>-1</sup>. The pH values were measured by a WTW pH meter. Conductivity was analyzed by the ISO 7888 method using a portable (WTW 340i) conductivity meter



with automatic temperature compensation, so that all results refer to 20 °C. All other parameters including turbidity and biological analysis were performed at the laboratory of the Institute Louis Pasteur in Douala.

## 2.5. Expression of Experimental Results

### 2.5.1. Value of E

To characterize the extent of the decontamination for individual contaminants (e.g., coliform, nitrate, turbidity), the effectiveness of the treatment (E) or attenuation percentage was calculated as follows (Equation (3)):

$$E = [1 - (C/C_0)] \times 100 \quad (3)$$

where C is the concentration after the experiment (residual effluent concentration), and  $C_0$  the initial aqueous concentration (initial influent concentration). The effectiveness comprises adsorption in the filter and possible other reactions that may occur during water throughput.

### 2.5.2. Hydraulic Conductivity

Changes of the hydraulic conductivity (permeability) were characterized by calculating the relative permeability “ $\phi$ ” (in%) at each filtration event using Equation (4):

$$\phi = 100 \times \phi/\phi_0 \quad (4)$$

where  $\phi_0$  is the initial value of the hydraulic conductivity and  $\phi$  its value at a later time.

## 3. Results and Discussion

### 3.1. Hydraulic Conductivity

Figure 2 and Table 3 (row 3) summarize the changes of relative filtration rate ( $\phi$ ) in the investigated filter. The results of a primary experiment for 6 months with a 50:50 Fe<sup>0</sup>/sand volumetric ratio (experiment 1) are also shown. It is seen that the filter in experiment 1 was not sustainable as an almost 90% permeability loss was observed [15]. The present experiment with a 10% Fe<sup>0</sup> (vol/vol) was designed accordingly (experiment 2). The results of experiment 1 depict the typical profile of permeability loss in Fe<sup>0</sup>-based filtration systems [17,49] with the  $\phi$  value dropping very abruptly. This behavior has been attributed to a local formation of a cake within the filter [50]. Clearly the system stays still mostly porous, but the inter-connectivity is suppressed in a domain where cake is formed. This is a testimony that the used Fe<sup>0</sup> ratio is too high [23].

The progressive decrease of the  $\phi$  values observed herein (40% in 12 months) was mainly attributed to iron corrosion. This assumption is supported by results of George and Ahammed [40] who performed similar experiments but with three individual systems (BSF and Fe<sup>0</sup>-amended BSF) for 4 months. The  $\phi$  values were 50.0%, 42.9%, and 15.6% for the systems Fe<sup>0</sup>-nails/sand, Fe<sup>0</sup>-scrap/sand, and BSF respectively. While George and Ahammed [40] are still speculating about the presence of Fe<sup>0</sup> as cause of decline in flow rate, the present study was designed to verify the textbook knowledge that iron corrosion is a volumetric expansive process [26], which implies that systems with lower Fe<sup>0</sup> ratios are more permeable [15,16,23,27,34].

**Table 3.** Characteristics of the effluent water over the testing period. The effluent iron concentration was constantly lower than the detection limit of the UV–Vis spectrophotometer ( $[\text{Fe}] < 0.2 \text{ mg L}^{-1}$ ).  $\phi$  is the water flow velocity.

t	pH	$\phi$	Total Coliforms	Turbidity	Nitrate
(d)	(-)	( $\text{L h}^{-1}$ )	(CFU/100 mL)	(NTU)	( $\text{mg L}^{-1}$ )
Raw water	4.9	0.0	1,950	35.0	24.0
1	6.6	20.0	0.11	1.09	0.21
15	6.7	20.0	0.11	1.07	0.19
30	6.6	20.0	0.11	1.00	0.20
45	6.8	20.0	0.10	1.00	0.20
60	6.8	19.6	0.10	1.01	0.15
75	6.9	19.6	0.10	1.00	0.15
90	6.7	18.8	0.10	0.99	0.12
105	6.6	18.8	0.08	0.80	<0.1
120	6.8	17.9	0.08	0.90	<0.1
135	7.0	17.5	0.08	0.90	<0.1
150	7.1	17.5	0.08	0.80	<0.1
165	7.3	17.1	0.08	0.80	<0.1
180	7.4	17.1	0.08	0.80	<0.1
195	7.5	16.7	0.02	0.90	<0.1
210	7.5	16.7	<0.02	0.90	<0.1
225	7.5	15.8	<0.02	0.80	<0.1
240	7.6	15.8	<0.02	0.90	<0.1
255	7.6	15.6	<0.02	0.90	<0.1
270	7.7	15.6	<0.02	0.80	<0.1
285	7.5	15.0	<0.02	0.80	<0.1
300	7.6	15.8	<0.02	0.70	<0.1
315	7.9	15.2	<0.02	0.80	<0.1
330	8.1	13.8	<0.02	0.70	<0.1
345	8.3	13.0	<0.02	0.80	<0.1
360	8.6	12.5	<0.02	0.70	<0.1

The design tested herein, a  $\text{Fe}^0$  SW filter sandwiched between two BSF filters, was an attempt to prolong the service life of the filter by consuming dissolved  $\text{O}_2$  in the first BSF, therefore operating under  $\text{O}_2$  low conditions and avoiding rapid system clogging [16,51]. The second BSF was used as Fe scavenger, to fix iron escaping from the  $\text{Fe}^0$  filter. The results of George and Ahammed [40] confirmed the  $\text{O}_2$  scavenging nature of both BSF and  $\text{Fe}^0$  filters. Mackenzie et al. [49] and Westerhoff and James [17] also used hybrid  $\text{Fe}^0$ /sand layers as  $\text{O}_2$  scavengers to sustain the efficiency of  $\text{Fe}^0/\text{H}_2\text{O}$  systems.

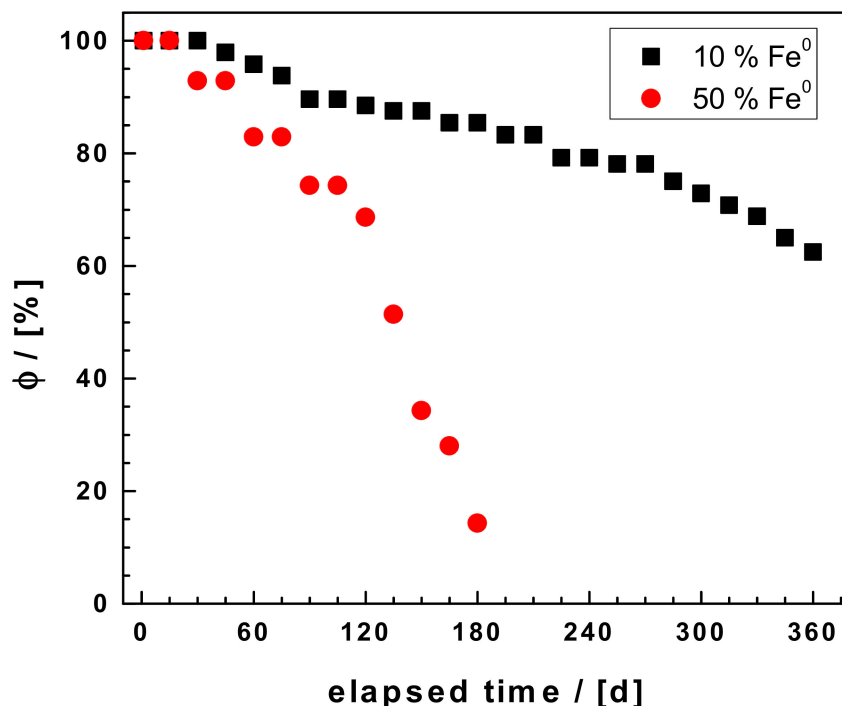


**Figure 2.** Flow rate variation over the length of filter runs for two different Fe<sup>0</sup> SW ratios (vol/vol): 50% and 10%. Experimental conditions: 800 g SW for 50% Fe<sup>0</sup> and 300 g SW for 10% Fe<sup>0</sup>; filling material: Sand. Column length: 100 cm, column diameter: 20 cm. The system was fed by natural well water polluted by fecal coliforms.

The qualitative similitude between this work and that of George and Ahammed [40] should not be overemphasized. This study used 300 g of Fe<sup>0</sup> SW making up a volumetric ratio of 10% while George and Ahammed [40] used 7.5 kg of mild steel nails and the same mass of scrap iron filing scrap uniformly mixed with sand throughout the reactive layer (Table 4). Given differences in key characteristics including density, form, intrinsic reactivity, and size, a quantitative comparison is difficult or even impossible. Obviously, under the respective operative conditions, the permeability loss at the end was acceptable.

The results achieved herein are more comparable to those of Bradley et al. [22]. The authors used a different grade of steel wool ( $d = 25 \mu\text{m}$  vs.  $50 \mu\text{m}$  herein) in the same volumetric percentage (10%) and reported on completed SW depletion after 170 days (almost 6 months). Upon Fe<sup>0</sup> depletion, the SW filter performed worse than the parallel operating BSF. This key observation was postulated by Noubactep et al. [51] and considered while designing the tested system [16]. In fact, O<sub>2</sub> depleted by Fe<sup>0</sup> is essential for the formation of the biofilm (Schmutzdecke), and pore filling by iron corrosion products have created preferential flow paths [52].

Lufingo [53] recently presented the first systematic characterization of Fe<sup>0</sup> SW specimens using their own developed tool (the Phen test). His results confirm the observed trends that neither the elemental composition, the size, or the surface state alone determine the kinetics and the extent of Fe<sup>0</sup> dissolution in aqueous solution [31]. However, because the pH value was still slightly increasing at the end of the experiment, it can be considered that SW was not depleted. Given that each natural water should be regarded as a unique system impacting the efficiency of Fe<sup>0</sup> filters [9], the results achieved herein are not easily transferable to other locations with different water quality. The authors suggest, however, that it is possible to design an efficient SW containing 10% Fe<sup>0</sup> (vol/vol) for use at household level. More systematic research is needed using, for example, the seven grades of Fe<sup>0</sup> SW characterized by Lufingo et al. [31] in combination with typical model waters representing the most common water sources (surface water, less and more saline groundwater) [34].



### 3.2. Turbidity Removal

Figure 3 and Table 3 (row 5) summarize the results of turbidity removal. The residual turbidity is listed, and the corresponding percent removal is depicted in Figure 3. The average influent turbidity was 35 NTU. The average effluent turbidity from the system was 0.7 NTU. The average turbidity removal efficiency from the influent was >97.99% during the experiment. This corroborates the results of George and Ahammed [40] and Bradley et al. [22] reporting about quantitative turbidity removal in both BSF and  $\text{Fe}^0$ -amended BSF. George and Ahammed [40] also reported that the amendment of  $\text{Fe}^0$  filters does not improve their turbidity removal efficiency. The results presented herein seem to confirm this assertion. However, this all depends on the design and the operational conditions. In essence,  $\text{Fe}^0$  amendment should improve turbidity removal because straining is improved by pore space reduction (expansive corrosion) [23].

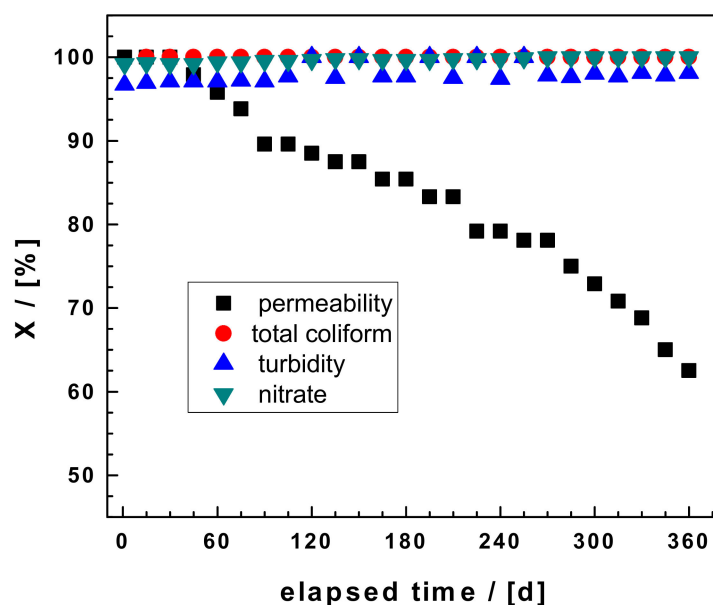


**Figure 3.** Permeability loss (percent) of the filter material and efficiencies of the removal of fecal coliform, turbidity, and nitrate (percent) in the effluent water over the length of filter run for the experiment with 10%  $\text{Fe}^0$  SW (vol/vol). Experimental conditions: 300 g SW; filling material: Sand; column length: 100 cm, column diameter: 20 cm. The system was fed by natural well water polluted by fecal coliform.

### 3.3. Nitrate Removal

Figure 3 and Table 3 (row 6) summarize the results of  $\text{NO}_3^-$  removal in the system. The corresponding percent removal is presented in Figure 3. The average influent  $\text{NO}_3^-$  concentration was  $23.5 \text{ mg L}^{-1}$ . Compared to the results of George and Ahammed [40], it is clear that  $\text{NO}_3^-$  removal mainly occurs in the  $\text{Fe}^0$  SW column. In fact, the authors spiked their influent solution with  $26.0 \text{ mg L}^{-1} \text{NO}_3^-$  and observed  $\text{NO}_3^-$  removal in all the three systems. The conventional BSF showed the lowest  $\text{NO}_3^-$  removal. The  $\text{NO}_3^-$  removal in BSF is well-documented, but the removal is never quantitative [54,55]. Thus, although the influent water used herein was not polluted by  $\text{NO}_3^-$  (Table 2), its removal was quantitative and occurred in the  $\text{Fe}^0$  SW column [17].

The mechanism of  $\text{NO}_3^-$  removal is complex and implies microbiological process in the BSF units [40,55] and both abiotic and biotic processes in the  $\text{Fe}^0$  SW unit [17,40].

### 3.4. pH Value and Iron Breakthrough

Table 3 gives the pH values (row 2) in the system's effluent. No iron breakthrough was observed ( $[\text{Fe}] < 0.2 \text{ mg L}^{-1}$ ). It is seen that the pH value progressively increased within the operational time and

reached 8.5 at the end of the experiments. The iron concentration was monitored to check whether any breakthrough occurred. The results showed that the second BSF quantitatively fixed iron for the whole duration of the experiment. Systems without scavenging BSF contain higher iron concentrations [17,56]. For example, Westerhoff and James [17] reported on up to  $6 \text{ mg L}^{-1}$  Fe in their effluent solutions. The very low iron concentration recorded herein is also in agreement with the pH dependent solubility of Fe hydroxides [57] as discussed for the “Fe<sup>0</sup> remediation” literature by Ghauch [58]. The fact that no iron breakthrough is observed herein suggests that the amount of iron (mainly Fe<sup>2+</sup>) escaping column 2 could not saturate the amount of sand in the second BSF. Fe<sup>2+</sup> is adsorbed onto sand by pure electrostatic interactions [46,59].

### 3.5. Removal of Coliform

Table 3 (row 4) and Figure 3 show reduction in total coliform concentration during the whole operation. There was a quantitative coliform removal already at the beginning of the experiment ( $E > 99.99\%$ ), and this trend kept through to the end (one year). This is due to three synergy processes: (i) formation of the biofilm in BSF, (ii) in situ generation of iron corrosion products (FeCPs), and (iii) reduction of the filtration rate. As discussed in Section 3.1, accumulation of FeCPs reduces the porosity and the permeability. They also improve coliform removal through adsorption [22,51]. It is essential to recall that the intrinsic bacterial inactivation capacity of Fe<sup>0</sup> was already reported in the 19th century [60–68] and has been independently demonstrated in the “Fe<sup>0</sup> remediation” research [69–74]. In the 19th century, quantitative pathogen removal in Fe<sup>0</sup> filters was demonstrated before the nature of individual bacteria was established. The diversity of microbiological populations in rivers and streams is obvious. On the contrary, current research efforts are demonstrating the efficiency of Fe<sup>0</sup> filters for pathogen removal on a case-by-case basis [75–78]. For example, You et al. [75] (re)demonstrated the suitability of Fe<sup>0</sup>/sand filters to inactivate waterborne viruses and refs. [76–78] tested the same (e.g., Fe<sup>0</sup>/sand filters) to remove various bacteria and viruses. Given that it is the dynamic process of aqueous iron corrosion which induces the remove all pathogens (Equations (1) and (2)), testing Fe<sup>0</sup>/sand filters on a case-by-case basis can be regarded superfluous [9].

**Table 4.** Summary of column dimension (length and diameter), the Fe<sup>0</sup> to sand ratio, the initial flow velocity ( $\phi_0$ ), the experimental duration (t), Fe<sup>0</sup> type, and the used Fe<sup>0</sup> mass of six selected peer-reviewed articles using column experiments for the removal of biological contamination. It is seen that one paper has not explicitly given the experimental duration. The authors of reference [77] used the number of pore volumes in their discussion. Two papers tested periods exceeding four months (120 days). In general, there is a large variability of the considered operational parameters.

L	D	Fe <sup>0</sup> /Sand	$\phi_0$	t	Fe <sup>0</sup> Type	m <sub>iron</sub>	Reference
(cm)	(cm)	(vol/vol)	(L h <sup>-1</sup> )	(d)	(-)	(kg)	
10	3.8	50:50	0.06	10	granular	0.15	[75]
20	n.s.	10:90	0.03	300	SW	0.26	[22]
0.77	0.14	50:50 *	n.s.	15	granular	23.0	[76]
10	3.8	50:50	4.38	n.s.	granular	n.s.	[77]
non SI	non SI	35:65	222	154	granular	n.s.	[78]
n.s.	n.s.	n.s.	n.s.	120	granular	7.5	[40]
100	20	10:90	20.4	365	SW	0.30	This study

\* is given in weight/weight; “n.s.” stands for not specified and “non SI” for units given in a not known system, for example “2” × 2 PVC plain-end pipe”.

### 3.6. Discussion

Previous studies testing contaminant removal from water by using Fe<sup>0</sup>-based column household water filters are numerous [9]. They were mostly designed to test diverse Fe<sup>0</sup> specimens for the removal

of selected contaminants [40] and/or to compare the efficiency of  $\text{Fe}^0$  filters to that of other systems, including BSFs [51]. As recently stated by Hu and Noubactep [24], available results demonstrate the suitability of  $\text{Fe}^0$  filters for water treatment. However, results from independent research are difficult to compare to each other. This section illustrates this difficulty based on selected references on the removal of pathogens from water. The six selected publications (Table 4) were not only focused on pathogen removal. They were selected to reflect the large diversity of reported experimental conditions. Achieved results are not addressed; the focus is on operational conditions as they are determinant for achieved results but are rarely considered while discussing achieved results [9].

Six operational parameters were selected for this discussion: (i) the column dimensions (D and L), (ii) the  $\text{Fe}^0$ /sand ratio, (iii) the initial flow velocity ( $F_0$ ), (iv) the experimental duration (t), (v) the  $\text{Fe}^0$  type, and (vi) the used  $\text{Fe}^0$  mass. It is seen that only  $\text{Fe}^0$ /sand ratio and the  $\text{Fe}^0$  type were specified by all six publications. The used volumetric  $\text{Fe}^0$  ratio varied between 10% and 50%, while  $\text{Fe}^0$  SW and granular materials were used. Concerning the column dimensions, small-scale columns and columns pertinent to pilot-scale tests were used while using flow velocities differing by more than three orders of magnitude. Lastly, 0.15 to 23 kg of  $\text{Fe}^0$  materials were used for operational duration varying from 10 to 365 days. There is no scientific basis to compare results from such experiments, particularly because the kinetics of iron corrosion are never linear, and the systems are dynamic in nature [24].

Table 4 clearly shows that a general weakness of the research projects undertaken to date on testing  $\text{Fe}^0$  systems for water treatment is that the long-term efficiency has not been investigated. Experiments designed for more than three months are in a large minority. This strategy is rather counter-intuitive in a context where long-term monitoring data are urgently needed [9,24,79].

### 3.7. Significance of the Results

$\text{Fe}^0$  materials have demonstrated their suitability for the design and dissemination of affordable, efficient, and sustainable safe drinking water provision systems over the past 170 years [3,10,11,14,61,62,80,81]. For the most recent success stories in decentralized systems, Hussam [11] used a proprietary material and Banerji and Chaudhari [14] used affordable iron nails. Progress in the large-scale realization of these and similar devices has been highly impeded by the lack of easy transferable designs. Using universally available steel wool ( $\text{Fe}^0$  SW) in this study was a step toward achieving universal access to safe drinking water [2,8,15,16,41,42].

Based on a concept presented by Noubactep et al. [8] and a mathematical model reasonably predicting optimal  $\text{Fe}^0$ /sand ratio for a sustainable filter [23,27], the present work has tested a volumetric  $\text{Fe}^0$ /sand ratio of 10:90 (300 g  $\text{Fe}^0$  SW) and obtained a filter that is able to treat natural well water polluted with pathogens for one year while depicting a permeability loss of only 40%. After one year the system was still capable of producing 200 L water per day, with an acceptable flow velocity ( $12.5 \text{ L h}^{-1}$ ). This water volume is far above the needs of an average family. If it is assumed that each person needs 7.5 L water per day for drinking and cooking, the designed filter can supply 25 people with safe drinking water, whether they are living in a small village, an urban slum, or a modern city. The filter is relatively easy in design; the most challenging task is homogeneously building the reactive zone, giving the huge difference in density between  $\text{Fe}^0$  SW and sand [22]. Herein, a dry packing approach in small lots was adopted. For future works, however, a wet packing approach as suggested by Sleiman et al. [82] should be tested. These authors pre-wetted the  $\text{Fe}^0$ /sand mixture to facilitate homogeneous  $\text{Fe}^0$  distribution in the column.

It should be insisted on that the most important result here is that a column containing 10% of  $\text{Fe}^0$  SW (vol/vol) or just 2% (w/w) and fed with natural water was still permeable after one year of operation. This result might not be reproduced by another  $\text{Fe}^0$  SW or a different water source, but the  $\text{Fe}^0$  ratio can be further decreased (and the column length increased) until a satisfactory balance is identified for each specific case. Sleiman et al. [82] used just 1% of  $\text{Fe}^0$  in their systems while Erickson et al. [33] hardly used more than 5% (w/w). Clearly, there is room for adjusting the operational conditions to any

site-specific situation. Where necessary, additional units made of affordable materials should be added to remove contaminants that are not well-addressed by  $\text{Fe}^0/\text{H}_2\text{O}$  systems [3,9,83].

#### 4. Conclusions

The results of the present study indicate a clear advancement in designing  $\text{Fe}^0$ -based household water units by rationally combining BSF and  $\text{Fe}^0$ /sand filters. By using a comparable volumetric  $\text{Fe}^0$ /SW ratio but a different  $\text{Fe}^0$  SW grade than Bradley et al. [22], a system still depicting acceptable permeability after one year was obtained. The designed system was able to convert a polluted well water into clean drinking water according to WHO standards. Considering that the duration of effective decontamination of  $\text{Fe}^0$ -based systems depends on both the water source and the nature of used  $\text{Fe}^0$ , the achieved results are highly qualitative. The achieved results call for further systematic research, which can start by duplicating the experiments reported herein with the seven grades of  $\text{Fe}^0$  SW from the same supplier.

Another field for future research is the characterization of the effects of typical water constituents on the efficiency of  $\text{Fe}^0$  SW filters. Relevant parameters include the presence of  $\text{Cl}^-$ ,  $\text{HCO}_3^-$ , humic substances,  $\text{SO}_4^{2-}$ , and  $\text{PO}_4^{3-}$ . The results of this study suggest that  $\text{Fe}^0$  SW filters are very affordable as only small amount of cheap SW (here 300 g) is required per household per year. Filter containers can be locally designed and constructed. A systematic approach for providing a chemistry-free, electricity-free barrier against waterborne diseases to millions of people based on SW filtration seems possible.

**Author Contributions:** The experiments were conceived and performed by R.T.-T., A.I.N.-T., A.N., H.R. and C.N. contributed equally to manuscript compilation and revisions.

**Funding:** This research received no external funding.

**Acknowledgments:** The manuscript was improved thanks to the insightful comments of anonymous reviewers from *Processes*. We acknowledge support by the German Research Foundation and the Open Access Publication Funds of the Göttingen University.

**Conflicts of Interest:** The authors declare no conflict of interest.

#### References

1. *Progress on Drinking Water, Sanitation and Hygiene-2017 Update and SDG Baselines*, WHO JMP launch version July 12 2017; WHO Library Cataloguing-in-Publication Data; WHO: Geneva, Switzerland, 2017. [CrossRef]
2. Nanseu-Njiki, C.P.; Gwenzi, W.; Pengou, M.; Rahman, M.A.; Noubactep, C.  $\text{Fe}^0/\text{H}_2\text{O}$  filtration systems for decentralized safe drinking water: Where to from here? *Water* **2019**, *11*, 429. [CrossRef]
3. Lauderdale, R.A.; Emmons, A.H. A method for decontaminating small volumes of radioactive water. *J. Am. Water Works Assoc.* **1951**, *43*, 327–331. [CrossRef]
4. Baig, S.A.; Mahmood, Q.; Nawab, B.; Shafqat, M.N.; Pervez, A. Improvement of drinking water quality by using plant biomass through household biosand filter—A decentralized approach. *Ecol. Eng.* **2011**, *37*, 1842–1848. [CrossRef]
5. Moglia, M.; Alexander, K.S.; Sharma, A. Discussion of the enabling environments for decentralised water systems. *Water Sci. Technol.* **2011**, *63*, 2331–2339. [CrossRef] [PubMed]
6. Hussam, A.; Munir, A.K.M. A simple and effective arsenic filter based on composite iron matrix: Development and deployment studies for groundwater of Bangladesh. *J. Environ. Sci. Health A* **2007**, *42*, 1869–1878. [CrossRef] [PubMed]
7. Ngai, T.K.K.; Murcott, S.; Shrestha, R.R.; Dangol, B.; Maharjan, M. Development and dissemination of Kanchan™ Arsenic Filter in rural Nepal. *Water Sci. Technol. Water Supply* **2006**, *6*, 137–146. [CrossRef]
8. Noubactep, C.; Schöner, A.; Wofo, P. Metallic iron filters for universal access to safe drinking water. *Clean Soil Air Water* **2009**, *37*, 930–937. [CrossRef]
9. Naseri, E.; Ndé-Tchoupé, A.I.; Mwakabona, H.T.; Nanseu-Njiki, C.P.; Noubactep, C.; Njau, K.N.; Wydra, K.D. Making  $\text{Fe}^0$ -based filters a universal solution for safe drinking water provision. *Sustainability* **2017**, *9*, 1224. [CrossRef]

10. Devonshire, E. The purification of water by means of metallic iron. *J. Frankl. Inst.* **1890**, *129*, 449–461. [[CrossRef](#)]
11. Hussam, A. Contending with a Development Disaster: SONO Filters Remove Arsenic from Well Water in Bangladesh. *Innovations* **2009**, *4*, 89–102. [[CrossRef](#)]
12. Henderson, A.D.; Demond, A.H. Impact of solids formation and gas production on the permeability of ZVI PRBs. *J. Environ. Eng.* **2011**, *137*, 689–696. [[CrossRef](#)]
13. Ngai, T.K.K.; Shrestha, R.R.; Dangol, B.; Maharjan, M.; Murcott, S.E. Design for sustainable development – Household drinking water filter for arsenic and pathogen treatment in Nepal. *J. Environ. Sci. Health A* **2007**, *42*, 1879–1888. [[CrossRef](#)] [[PubMed](#)]
14. Banerji, T.; Chaudhari, S. A cost-effective technology for arsenic removal: Case study of zerovalent iron-based iit bombay arsenic filter in west bengal. In *Water and Sanitation in the New Millennium*; Nath, K., Sharma, V., Eds.; Springer: New Delhi, India, 2017.
15. Tepong-Tsindé, R. Metallic Iron Filters for Safe Drinking Water in Informal Settlements of Douala (Cameroun): A Pilot Scale Study. Ph.D. Thesis, University of Göttingen, Göttingen, Germany, 2020.
16. Tepong-Tsindé, R.; Crane, R.; Noubactep, C.; Nassi, A.; Ruppert, H. Testing metallic iron filtration systems for decentralized water treatment at pilot scale. *Water* **2015**, *7*, 868–897. [[CrossRef](#)]
17. Westerhoff, P.; James, J. Nitrate removal in zero-valent iron packed columns. *Water Res.* **2003**, *37*, 1818–1830. [[CrossRef](#)]
18. Ahammed, M.M.; Davra, K. Performance evaluation of biosand filter modified with iron oxide-coated sand for household treatment of drinking water. *Desalination* **2011**, *276*, 287–293. [[CrossRef](#)]
19. Haig, S.J.; Collins, G.; Davies, R.L.; Dorea, C.C.; Quince, C. Biological aspects of slow sand filtration: Past, present and future. *Water Sci. Technol. Water Supply* **2011**, *11*, 468–472. [[CrossRef](#)]
20. Nitzsche, K.S.; Lan, V.M.; Trang, P.T.K.; Viet, P.H.; Berg, M.; Voegelin, A.; Planer-Friedrich, B.; Zahoransky, J.; Müller, S.-K.; Byrne, J.M.; et al. Arsenic removal from drinking water by a household sand filter in Vietnam—Effect of filter usage practices on arsenic removal efficiency and microbiological water quality. *Sci. Total Environ.* **2015**, *502*, 526–536. [[CrossRef](#)]
21. Jia, Y.; Aagaard, P.; Breedveld, G.D. Sorption of triazoles to soil and iron minerals. *Chemosphere* **2007**, *67*, 250–258. [[CrossRef](#)]
22. Bradley, I.; Straub, A.; Maraccini, P.; Markazi, S.; Nguyen, T.H. Iron oxide amended biosand filters for virus removal. *Water Res.* **2011**, *45*, 4501–4510. [[CrossRef](#)]
23. Domga, R.; Togue-Kamga, F.; Noubactep, C.; Tchatchueng, J.B. Discussing porosity loss of Fe<sup>0</sup> packed water filters at ground level. *Chem. Eng. J.* **2015**, *263*, 127–134. [[CrossRef](#)]
24. Hu, R.; Noubactep, C. Redirecting research on Fe<sup>0</sup> for environmental remediation: The search for synergy. *Int. J. Environ. Res. Public Health* **2019**, *16*, 4465. [[CrossRef](#)] [[PubMed](#)]
25. Pilling, N.B.; Bedworth, R.E. The oxidation of metals at high temperatures. *J. Inst. Met.* **1923**, *29*, 529–591.
26. Landolt, D. *Corrosion and Surface Chemistry of Metals*, 1st ed.; EPFL Press: Lausanne, Switzerland, 2007; p. 615.
27. Caré, S.; Crane, R.; Calabrò, P.S.; Ghauch, A.; Temgoua, E.; Noubactep, C. Modeling the permeability loss of metallic iron water filtration systems. *CLEAN Soil Air Water* **2013**, *41*, 275–282. [[CrossRef](#)]
28. Moraci, N.; Lelo, D.; Bilardi, S.; Calabrò, P.S. Modelling long-term hydraulic conductivity behaviour of zero valent iron column tests for permeable reactive barrier design. *Can. Geotech. J.* **2016**, *53*, 946–961. [[CrossRef](#)]
29. Noubactep, C. Predicting the hydraulic conductivity of metallic iron filters: Modeling gone astray. *Water* **2016**, *8*, 162. [[CrossRef](#)]
30. Hammonds, P. An Introduction to Corrosion and its Prevention (Chapter 4). *Compr. Chem. Kinet.* **1989**, *28*, 233–279.
31. Lufingo, M.; Ndé-Tchoupé, A.I.; Hu, R.; Njau, K.N.; Noubactep, C. A novel and facile method to characterize the suitability of metallic iron for water treatment. *Water* **2019**, *11*, 2465. [[CrossRef](#)]
32. Wakatsuki, T.; Esumi, H.; Omura, S. High performance and N, P removable on-site domestic wastewater treatment system by multi-soil-layering method. *Water Sci. Technol.* **1993**, *27*, 31–40. [[CrossRef](#)]
33. Erickson, A.J.; Gulliver, J.S.; Weiss, P.T. Phosphate removal from agricultural tile drainage with iron enhanced sand. *Water* **2017**, *9*, 672. [[CrossRef](#)]
34. Luo, P.; Bailey, E.H.; Mooney, S.J. Quantification of changes in zero valent iron morphology using X-ray computed tomography. *J. Environ. Sci.* **2013**, *25*, 2344–2351. [[CrossRef](#)]



35. Özer, A.; Altundogan, H.S.; Erdem, M.; Tümen, F. A study on the Cr (VI) removal from aqueous solutions by steel wool. *Environ. Pollut.* **1997**, *97*, 107–112. [[CrossRef](#)]
36. Campos, V. The effect of carbon steel-wool in removal of arsenic from drinking water. *Environ. Geol.* **2002**, *42*, 81–82. [[CrossRef](#)]
37. Cornejo, L.; Lienqueo, H.; Arenas, M.; Acarapi, J.; Contreras, D.; Yáñez, J.; Mansilla, H.D. In field arsenic removal from natural water by zero-valent iron assisted by solar radiation. *Environ. Pollut.* **2008**, *156*, 827–831. [[CrossRef](#)]
38. Triszcz, J.M.; Porta, A.; Einschlag, F.S.G. Effect of operating conditions on iron corrosion rates in zero-valent iron systems for arsenic removal. *Chem. Eng. J.* **2009**, *150*, 431–439. [[CrossRef](#)]
39. Rao, T.S.; Murthy, D.S. Removal of arsenic (V) from water by adsorption onto low-cost and waste materials. *Int. J. Res. Eng. Technol.* **2013**, *2*, 206–212.
40. George, D.; Ahammed, M.A. Effect of zero-valent iron amendment on the performance of biosand filters. *Water Supply* **2019**, *19*, 1612–1618. [[CrossRef](#)]
41. Ndé-Tchoupé, A.I.; Crane, R.A.; Mwakabona, H.T.; Noubactep, C.; Njau, K.N. Technologies for decentralized fluoride removal: Testing metallic iron based filters. *Water* **2015**, *7*, 6750–6774. [[CrossRef](#)]
42. Ndé-Tchoupé, A.I. Design and Construction of Fe<sup>0</sup>-Based Filters for Households. Ph.D. Thesis, University of Douala, Douala, Cameroon, 2019. (In French).
43. Varlikli, C.; Bekiari, V.; Kus, M.; Boduroglu, N.; Oner, I.; Lianos, P.; Lyberatos, G.; Icli, S. Adsorption of dyes on Sahara desert sand. *J. Hazard. Mater.* **2009**, *170*, 27–34. [[CrossRef](#)]
44. James, B.R.; Rabenhorst, M.C.; Frigon, G.A. Phosphorus sorption by peat and sand amended with iron oxides or steel wool. *Water Environ. Res.* **1992**, *64*, 699–705. [[CrossRef](#)]
45. Chiew, H.; Sampson, M.L.; Huch, S.; Ken, S.; Bostick, B.C. Effect of groundwater iron and phosphate on the efficacy of arsenic removal by iron-amended biosand filters. *Environ. Sci. Technol.* **2009**, *43*, 6295–6300. [[CrossRef](#)]
46. Btateu-K, B.D.; Olvera-Vargas, H.; Tchatchueng, J.B.; Noubactep, C.; Caré, S. Determining the optimum Fe<sup>0</sup> ratio for sustainable granular Fe<sup>0</sup>/sand water filters. *Chem. Eng. J.* **2014**, *247*, 265–274. [[CrossRef](#)]
47. Saywell, L.G.; Cunningham, B.B. Determination of iron: Colorimetric o-phenanthroline method. *Ind. Eng. Chem. Anal. Ed.* **1937**, *9*, 67–69. [[CrossRef](#)]
48. Fortune, W.B.; Mellon, M.G. Determination of iron with o-phenanthroline. *Ind. Eng. Chem. Anal. Ed.* **1938**, *10*, 60–64. [[CrossRef](#)]
49. Mackenzie, P.D.; Horney, D.P.; Sivavec, T.M. Mineral precipitation and porosity losses in granular iron columns. *J. Hazard. Mater.* **1999**, *68*, 1–17. [[CrossRef](#)]
50. Santisukksaem, U.; Das, D.B. A non-dimensional analysis of permeability loss in zero-valent iron permeable reactive barrier (PRB). *Transp. Porous Media* **2019**, *126*, 139–159. [[CrossRef](#)]
51. Noubactep, C.; Temgoua, E.; Rahman, M.A. Designing iron-amended biosand filters for decentralized safe drinking water provision. *CLEAN Soil Air Water* **2012**, *40*, 798–807. [[CrossRef](#)]
52. Miyajima, K. Optimizing the design of metallic iron filters for water treatment. *Freib. Online Geosci.* **2012**, *32*, 1–60.
53. Lufingo, M. Investigation of Metallic Iron for Water Defluoridation. Master's Thesis, Nelson Mandela African Institution of Science and Technology, Arusha, Tanzania, 2019.
54. Nakhla, G.; Farooq, S. Simultaneous nitrification–denitrification in slow sand filters. *J. Hazard. Mater.* **2003**, *96*, 291–303. [[CrossRef](#)]
55. Murphy, H.M.; McBean, E.A.; Farahbakhsh, K. Nitrification, denitrification and ammonification in point-of-use biosand filters in rural Cambodia. *J. Water Health* **2010**, *8*, 803–817. [[CrossRef](#)]
56. Heimann, S.; Ndé-Tchoupé, A.I.; Hu, R.; Licha, T.; Noubactep, C. Investigating the suitability of Fe<sup>0</sup> packed-beds for water defluoridation. *Chemosphere* **2018**, *209*, 578–587. [[CrossRef](#)]
57. Liu, X.; Millero, F.J. The solubility of iron hydroxide in sodium chloride solutions. *Geochim. Cosmochim. Acta* **1999**, *63*, 3487–3497. [[CrossRef](#)]
58. Ghauch, A. Iron-based metallic systems: An excellent choice for sustainable water treatment. *Freib. Online Geosci.* **2015**, *32*, 1–80.
59. Btateu-K, B.D.; Olvera-Vargas, H.; Tchatchueng, J.B.; Noubactep, C.; Caré, S. Characterizing the impact of MnO<sub>2</sub> on the efficiency of Fe<sup>0</sup>-based filtration systems. *Chem. Eng. J.* **2014**, *250*, 416–422. [[CrossRef](#)]



60. Bischof, G. Über das Reinigen des Wassers und über die Wirkung des Eisenschwammes auf unreines Wasser. *Polytech. J.* **1873**, *210*, 40–59.
61. Bischof, G. On putrescent organic matter in potable water. *Proc. R. Soc. Lond.* **1877**, *26*, 258–261.
62. Bischof, G. On putrescent organic matter in potable water II. *Proc. R. Soc. Lond.* **1878**, *27*, 152–156.
63. Notter, J.L. The purification of water by filtration. *Br. Med. J.* **1878**, *Oct. 12*, 556–557. [[CrossRef](#)]
64. Hatton, F. On the oxidation of organic matter in water by filtration through various media; and on the reduction of nitrates by sewage, spongy iron, and other agents. *J. Chem. Soc. Trans.* **1881**, *39*, 258–276. [[CrossRef](#)]
65. Bache, R.M. Possible sterilization of city water. *Proc. Am. Philos. Soc.* **1891**, *29*, 26–39.
66. Leffmann, H. The purification of water by metallic iron. In Proceedings of the 11th Annual Meeting of the American Water Works Association, Philadelphia, PA, USA, 14–16 April 1991; pp. 163–171.
67. Tweeddale, W. Water purification. *Trans. Ann. Meet. Kans. Acad. Sci.* **1898**, *16*, 48–52. [[CrossRef](#)]
68. Baker, M.N. Sketch of the history of water treatment. *J. Am. Water Works Assoc.* **1934**, *26*, 902–938. [[CrossRef](#)]
69. Bojic, A.; Purenovic, M.; Kocic, B.; Perovic, J.; Ursic-Jankovic, J.; Bojic, D. The inactivation of escherichia coli by microalloyed aluminium based composite. *Facta Univ. Phys. Chem. Technol.* **2001**, *2*, 115–124.
70. Lee, C.; Kim, J.H.; Lee, W.I.; Nelson, K.L.; Yoon, J.; Sedlak, D.L. Bactericidal effect of zero-valent iron nanoparticles on escherichia coli. *Environ. Sci. Technol.* **2008**, *42*, 4927–4933. [[CrossRef](#)] [[PubMed](#)]
71. Diao, M.; Yao, M. Use of zero-valent iron nanoparticles in inactivating microbes. *Water Res.* **2009**, *43*, 5243–5251. [[CrossRef](#)]
72. Crampon, M.; Joulain, C.; Ollivier, P.; Charron, M.; Hellal, J. Shift in natural groundwater bacterial community structure due to zero-valent iron nanoparticles (nZVI). *Front. Microbiol.* **2019**, *10*, 533. [[CrossRef](#)]
73. Hu, Y.; Wang, J.; Sun, H.; Wang, S.; Liao, X.; Wang, J.; An, T. Roles of extracellular polymeric substances in the bactericidal effect of nanoscale zero-valent iron: Trade-offs between physical disruption and oxidative damage. *Environ. Sci. Nano* **2019**, *6*, 2061–2073. [[CrossRef](#)]
74. Sun, H.; Wang, J.; Jiang, Y.; Shen, W.; Jia, F.; Wang, S.; Liao, X.; Zhang, L. Rapid aerobic inactivation and facile removal of escherichia coli with amorphous zero-valent iron microspheres: Indispensable roles of reactive oxygen species and iron corrosion products. *Environ. Sci. Technol.* **2019**, *53*, 3707–3717. [[CrossRef](#)]
75. You, Y.; Han, J.; Chiu, P.C.; Jin, Y. Removal and inactivation of waterborne viruses using zerovalent iron. *Environ. Sci. Technol.* **2005**, *39*, 9263–9269. [[CrossRef](#)]
76. Ingram, D.T.; Callahan, M.T.; Ferguson, S.; Hoover, D.G.; Shelton, D.R.; Millner, P.D.; Camp, M.J.; Patel, J.R.; Kniel, K.E.; Sharma, M. Use of zero-valent iron biosand filters to reduce E. coli O157:H12 in irrigation water applied to spinach plants in a field setting. *J. Appl. Microbiol.* **2012**, *112*, 551–560. [[CrossRef](#)]
77. Shi, C.; Wei, J.; Jin, Y.; Kniel, K.E.; Chiu, P.C. Removal of viruses and bacteriophages from drinking water using zero-valent iron. *Sep. Purif. Technol.* **2012**, *84*, 72–78. [[CrossRef](#)]
78. Marik, C.M.; Anderson-Coughlin, B.; Gartley, S.; Craighead, S.; Kniel, K.E. The efficacy of zero valent iron-sand filtration on the reduction of Escherichia coli and Listeria monocytogenes in surface water for use in irrigation. *Environ. Res.* **2019**, *173*, 33–39. [[CrossRef](#)] [[PubMed](#)]
79. Hu, R.; Gwenzi, G.; Sipowo, R.; Noubactep, C. Water treatment using metallic iron: A tutorial review. *Processes* **2019**, *7*, 622. [[CrossRef](#)]
80. Tucker, W.G. The purification of water by chemical treatment. *Science* **1892**, *20*, 34–38. [[CrossRef](#)] [[PubMed](#)]
81. Mwakabona, H.T.; Ndé-Tchoupé, A.I.; Njau, K.N.; Noubactep, C.; Wydra, K.D. Metallic iron for safe drinking water provision: Considering a lost knowledge. *Water Res.* **2017**, *117*, 127–142. [[CrossRef](#)] [[PubMed](#)]
82. Sleiman, N.; Deluchat, V.; Wazne, M.; Mallet, M.; Courtin-Nomade, A.; Kazpard, V.; Baudu, M. Phosphate removal from aqueous solution using ZVI/sand bedreactor: Behavior and mechanism. *Water Res.* **2016**, *99*, 56–65. [[CrossRef](#)]
83. Gwenzi, W.; Chaukura, N.; Noubactep, C.; Mukome, F.N.D. Biochar-based water treatment systems as a potential low-cost and sustainable technology for clean water provision. *J. Environ. Manag.* **2017**, *197*, 732–749. [[CrossRef](#)]

